Key Engineering Materials
ISSN: 1662-9795, Vol. 926, pp 1143-1150
doi:10.4028/p-05e2kr

Submitted: 2022-01-24
Revised: 2022-01-27
Accepted: 2022-02-25
Online: 2022-07-22

Near-Net Forging of Titanium and Titanium Alloys by the Plasma Carburized SKD11 Dies

Tatsuhiko Aizawa[1,a], Shunsuke Ishiguro[2,b], Tomomi Shiratori[2,c,*] and Tomoaki Yoshino[3,d]

[1]3-15-10 Minami-Rokugo, Ota-City, Tokyo 144-0045, Japan

[2]Gofuku, Toyama-City, Toyama 930-8555, Japan

[3]Shiga-Kuwahara, Suwa-City, Nagano 392-0012, Japan

[a]taizawa@sic.shibaura-it.ac.jp, [b]m1971202@ems.u-toyama.ac.jp, [c,*]shira@eng.u-toyama.ac.jp, [d]yoshino@komatsuseiki.co.jp

Keywords: Carbon supersaturated SKD11 dies, titanium wires, forging, in situ solid lubrication

Abstract. The carbon supersaturated SKD11 punch and core-die were prepared by the plasma carburizing at 673 K for 14.4 ks. The upsetting experiment was performed by using this punch to describe the plastic flow of pure titanium and β-titanium works in higher reduction of thickness than 50%. The measured load – stroke relationship was utilized to describe the frictional behavior on the contact interface of punch to work materials and their work hardening process. The contact interface of carbon supersaturated punch to work was analyzed to investigate the formation of isolated carbon tribofilms from punch material and to describe the in situ solid lubrication on the contact interface. The micro-hardness mapping technique was also utilized to investigate how to suppress the work-hardening behavior by this in-situ solid lubrication. Free near-net forging experiments were performed to shape the circular β-titanium alloy wires to triangular bars.

Introduction

Titanium and titanium alloys have been high-lighted as a structural member of aircrafts [1], a biomedical tool [2], a sporting goods [3], a mechanical part of watches, robots, MEMS [4] and so forth. Their high strength and light-weight are all attractive to mechanical designers but their difficulty in metal forming hinders this possibility. In particular, their fresh surfaces appear during their forging and forge-stamping processes and often adhere to the die surfaces [5]. This mass adhesion or the chemical galling to the die and tool becomes the most essential issue in their engineering and medical applications.

This difficulty was solved by innovative change of die substrate materials. The β-SiC coated SiC die with carbon supersaturation (cs) was proposed as a punch and core-die material for galling free forging of titanium and titanium alloys [6-10]. The isolated carbon dots and agglomerates from the cs-β-SiC coating wrought as a solid lubricant on the highly stressed contact interface together with the intermediate titanium oxide tribofilms. Since β-SiC has high heat resistance at the highly elevated temperature, this approach becomes effective even in warm and hot forging and stamping processes. Its effectiveness in near-net shaping is limited in nature because of its low toughness [11-12]. The low temperature plasma carburized steel dies were proposed as the second approach to the galling-free forging [13-15]. In similar manner to the cs-β-SiC coating dies, the free carbon isolates from the cs-SKD11 dies and forms a carbon-stripe tribofilm onto their contact interface to titanium and titanium alloy works. Due to the higher hardness than 1200 HV and its original ductility and toughness, this approach is available in almost all the forming processes in the technology of plasticity.

In the present paper, the pure titanium and β-titanium alloy wires with the diameter of 3 mm are employed to demonstrate their workability in the upsetting and near-net shaping processes. The plasma carburized SKD11 punch and core-die are prepared by the low temperature plasma carburizing. An upsetting experiment is performed to describe the plastic flow with increasing the

reduction of thickness (r). This contact interface is analyzed by SEM (Scanning Electron Microscopy) – EDX (Electron Diffractive X-ray spectroscopy) and Raman spectroscopy to demonstrate the in situ formation of free carbon tribofilms on the interface. The micro-hardness mapping technique is also employed to investigate how to suppress the work-hardening of pure titanium and β-titanium by the in situ solid lubrication. In a free-forging experiment, a circular wire is precisely shaped into a triangular bar by filling into a groove of core die. Variation of shaped wire geometry with increasing r is observed and analyzed to describe the frictional behavior on the contact interface of punch to wire.

Experimental Procedure

Low temperature plasma carburizing system. A radio frequency (RF)–direct current (DC) plasma carburizing system (CVD-I, YS-Electric Industry, Co., Ltd., Koufu Japan) was employed in this study with the use of the hollow cathode device. In the following experiments, a mixture gas of argon and hydrogen with the flow rate ratio of 100 mL/min to 80 mL/min was introduced to a chamber for presputtering after evacuating, filling the chamber with argon and heating to the holding temperature of 673 K. This presputtering for 1.8 ks (0.5 h) at 673 K in 70 Pa was followed by the plasma carburizing at 673 K, in 70Pa for 14.4 ks (4 h) after introducing CH_4 gas by 20 mL/min. In this carburizing process, RF–voltage and DC–bias, were constant by 200 V and −600 V, respectively. After carburizing, the chamber was evacuated and cooled down in a nitrogen atmosphere. Figure 1a illustrates an experimental setup for this plasma carburizing. As shown in Figure 1b, the SKD11 punch and core-die were surrounded by the plasma sheath with high population of carbon ions and CH-radicals.

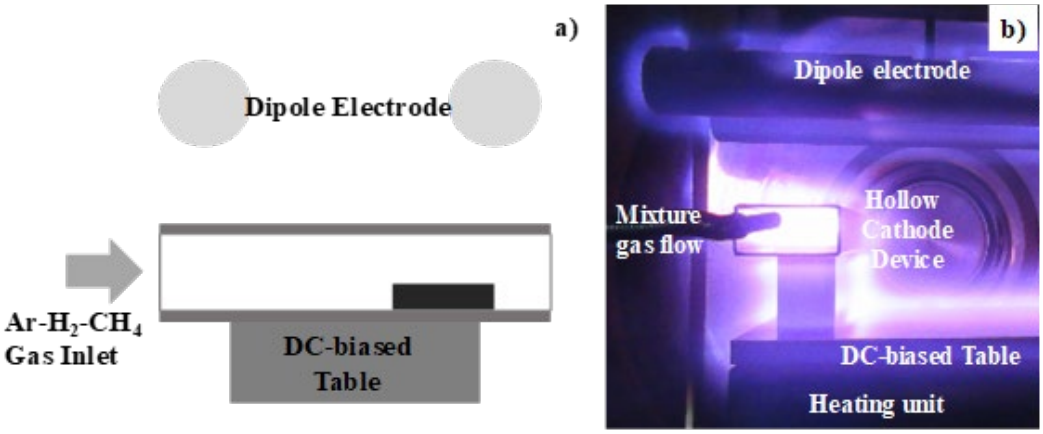

Figure 1. A plasma carburizing system working at 673 K for 14.4 ks. a) A schematic view of experimental setup including the hollow cathode device, and b) a snap-shot view of confined plasma sheath into the hollow cathode.

Two types of SKD11 dies were prepared for this plasma carburizing process. A SKD11 punch with its head size of 20 mm x 10 mm was plasma-carburized and polished with the use of diamond paste. A SKD11 core-die with the triangular groove was also plasma carburized under the same conditions as processing the above SKD11 punch. The cs-SKD11 punch and core-die were cleaned by the ultrasonic cleaner to eliminate any surfactants. In XRD analysis, the original α-iron peak (110) shifted to the lower 2θ side. The original bcc (body-center cubic) crystallographic cell expands itself by the carbon supersaturation. In addition to this peak shift, the expanded austenitic phase is also detected in the XRD diagram. As reported in [14], the austenitic phase transformation takes place with the carbon supersaturation into SKD11 punch and die.

Upsetting and near-net forging system. In the upsetting experiments with high reduction of thickness, the cs-SKD11 punch and the cs-β-SiC die were employed to describe the low friction and galling-free plastic flow of pure titanium and β-titanium wires with the diameter of 3 mm. The

hardness mapping technique [16] was employed to describe the work-hardening behavior in upsetting the works with increasing the reduction of thickness.

In the near-net forging experiment, both the cs-SKD11 punch and core-die were respectively fixed into the upper and lower cassette die-sets. CNC (Computer Numerical Control) stamping system in Figure 2a was employed for free forging to shape a circular wire to a triangular bar. Figure 2b depicts the upper cassette die-set which is cemented to the upper bolster of stamper. The load – stroke relationship was in-line monitored during this free forging experiment. The stroke was defined by the linear-scale positioning sensor. The applied load was measured by the load-cell, which was embedded into the lower cassette die-set.

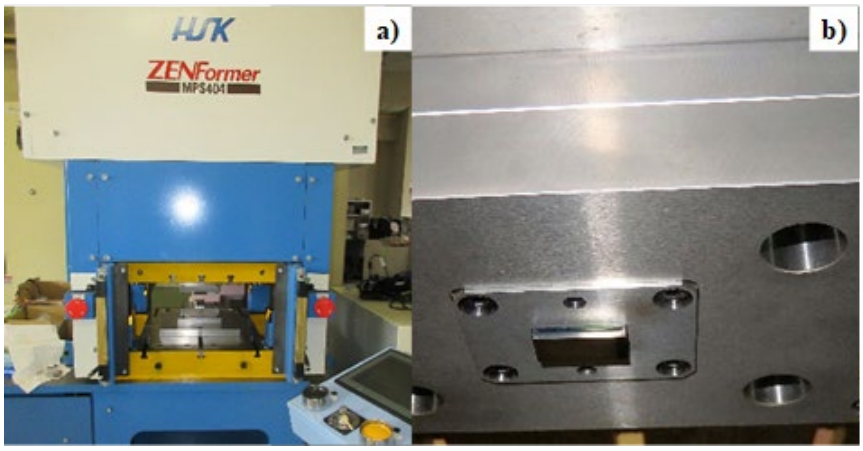

Figure 2. CNC-stamping system and die-setting for free forging experiments. a) Overview of the CNC-stamper with the upper and lower cassette dies, and b) normal setting of the carburized SKD11 punch into the upper cassette die-set.

Material characterization. SEM – EDX system (JOEL; Tokyo, Japan) was utilized to make microstructure analysis on the contact interface of cs-SKD11 punch to pure titanium and b-phase titanium wires after continuously forging these works by 10 shots. The region to be analyzed on the interface was determined by the optical microscopy observation. In EDX, the energy profile was first measured to identify the constituent elements of the tribofilm on the contact interface.

Experimental Results and Discussion

Upsetting and near net shaping processes of pure titanium and β-titanium wires are described with increasing the reduction ratio (r) of thickness. The bulging deformation ratio and the hardness mapping are employed as a parameter to analyze the friction on the contact interface and the work hardening behavior, respectively.

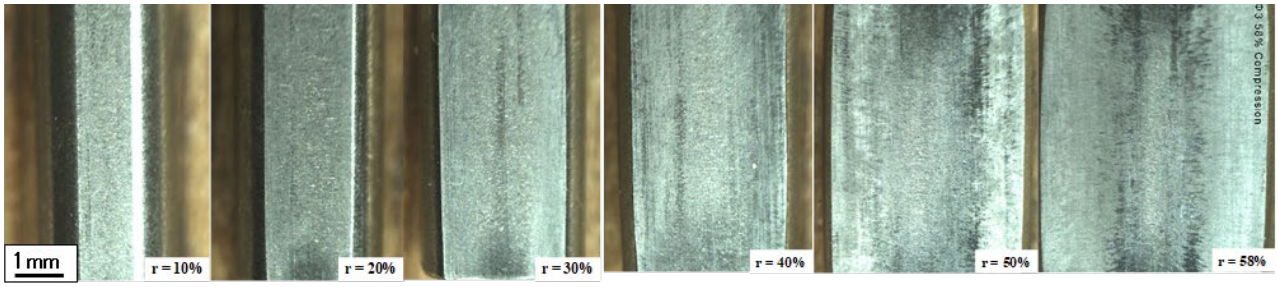

Figure 3. Upsetting behavior of β-titanium wire with the initial diameter of 3.0 mm (D_0 = 3 mm) with increasing the reduction of thickness (r) up to 58%.

High reduction upsetting of pure titanium and β-titanium wires. The cs-SKD11 punch and β-SiC coated SiC die were fixed respectively into the upper and lower cassette dies for this upsetting experiments. Figure 3 depicts the flattening behavior of β-titanium wire with increasing r. When r > 30%, the contact interface width (Wi) approaches to the flattening wire width (Wo); the bulging

deformation (B_g= (Wo-Wi)/2) is significantly reduced. After [17], this little non-dimensional bulging deformation proves the friction coefficient (μ) remains 0.05 to 0.1 on the contact interface of cs-SKD11 punch to the β-Ti work.

The ratio (R_W) of Wi to D_0, is employed as a parameter to describe the plastic formability. Table 1 lists these R_W, Wi, Wo and B_g at each r for the pure titanium and β-titanium, respectively. Monotonic increase of R_w and monotonous decrease of B_g with increasing r for two titanium works reveal that the flattening process advances with r in low friction interface condition. R_W = 1.35 for pure titanium and R_W = 1.42 for β-titanium at r = 50%; the work-hardening with increasing r is lower in upsetting the β-titanium.

Table 1. Variation of Wi, Wo, B_g and R_W with increasing r during upsetting the pure titanium and β-titanium wires with the initial diameter of 3 mm.

	Pure Titanium Work				**β-Titanium Work**			
r (%)	R_W (--)	Wi (mm)	Wo (mm)	Bg (mm)	R_W (--)	Wi (mm)	Wo (mm)	B_g (mm)
0	0.00	0.00	3.00	---	0.00	0.00	3.00	---
10	0.38	1.13	3.01	0.94	0.38	1.15	3.07	0.96
20	0.61	1.82	3.20	0.69	0.62	1.85	3.24	0.70
30	0.86	2.59	3.59	0.50	0.89	2.68	3.63	0.48
40	1.03	3.08	3.94	0.43	1.13	3.38	4.06	0.34
50	1.35	4.05	4.64	0.30	1.42	4.27	4.70	0.22
58	1.71	5.14	5.58	0.22	1.68	5.04	5.43	0.20

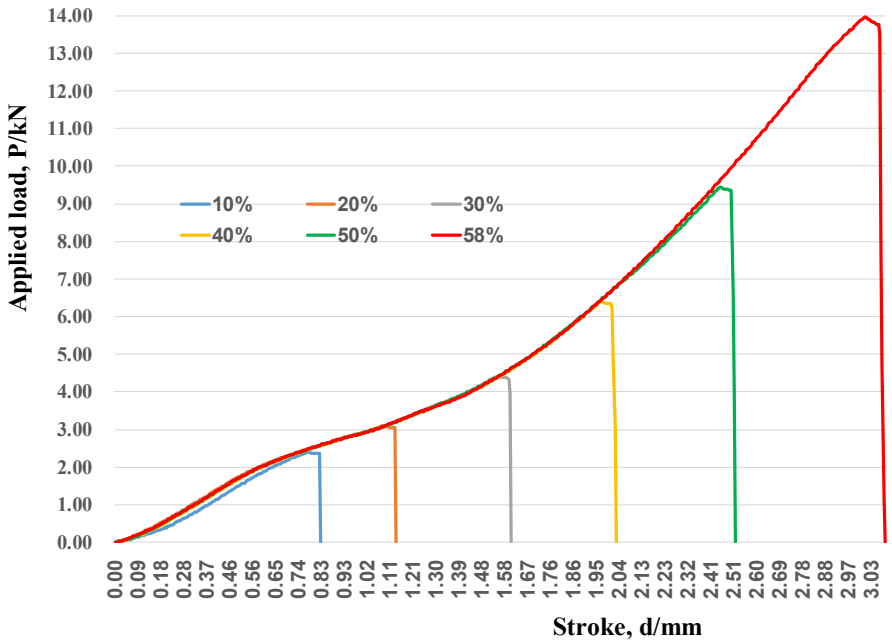

Figure 4. Relationship of the applied load (P) to the stroke (d) during upsetting the β-titanium wire.

At every reduction of thickness, the load – stroke relation was monitored during upsetting the β-titanium wires. As shown in Figure 4, the measured six relations were edited to a single master P – d curve. For r > 20%, the load monotonously increases with d due to the flattening plastic flow on the interface. At each r, the contact area (A_r) of cs-SKD11 punch to work was estimated to calculate the average applied stress (σ) by $\sigma = P/A_r$. Table 2 describes the variation of measured P, Ar and estimated s with r for two titanium works.

Table 2. Variation of the measured load (P), contact area (A_r) and calculated stress (s) with increasing r during upsetting the pure and β-phase titanium wires.

	Pure Titanium Work			**β-Titanium Work**		
r (%)	P (kN)	A_r (mm^2)	σ (MPa)	P (kN)	A_r (mm^2)	σ (MPa)
0	0.00	0.00	0.00	0.00	0.00	0.00
10	2.02	10.28	196	2.37	10.92	217
20	3.14	17.16	183	3.10	---	---
30	5.22	27.49	190	4.41	---	---
40	6.64	31.74	209	6.39	32.97	194
50	10.49	43.90	239	9.44	42.13	224
58	15.86	56.24	282	13.94	52.61	265

The stress transient for r > 30% in upsetting the β-titanium remains lower than that in upsetting the pure titanium. This also proves that the work hardening process is more suppressed by using the b-titanium works.

Micro-Hardness Mapping. The micro-hardness mapping technique was employed to describe the work hardening behavior in upsetting the pure and β-phase titanium wires. The bulging behavior and shear localization process in upsetting are much dependent on the friction on the contact interface. Under the highly frictional interface, a wire-work bulges in the plain strain condition with severe shear localization on its cross-section. On the other hand, little bulging with less strain localization takes place even with increasing the reduction of thickness [18].

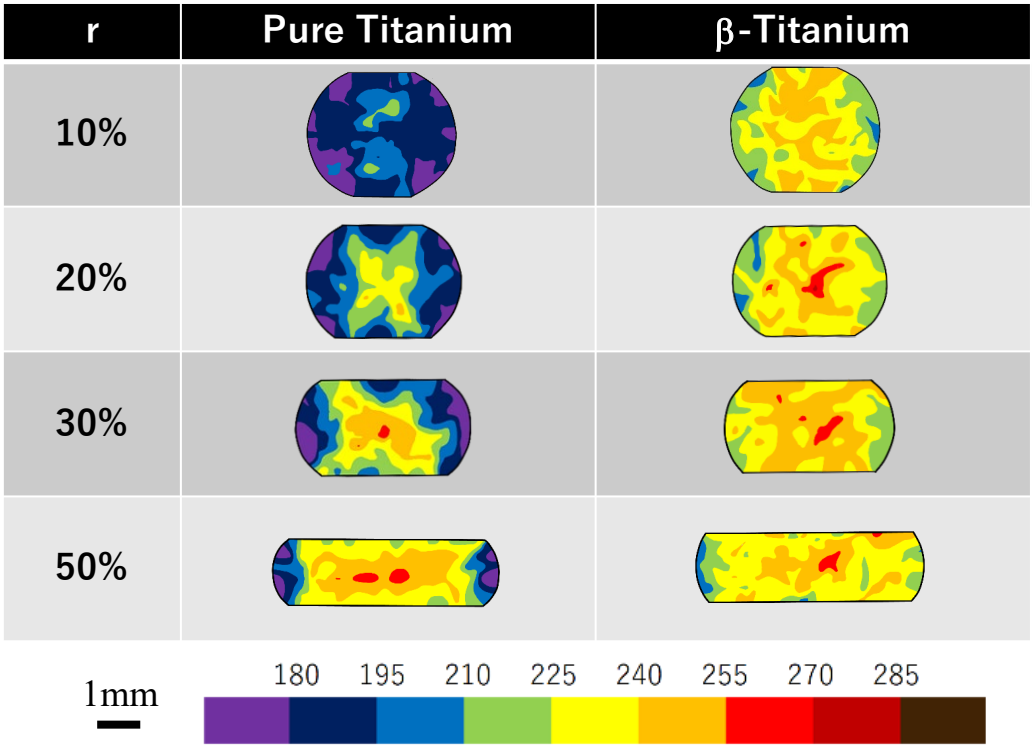

Figure 5. Comparison of micro-hardness mapping between the pure and β-phase titanium works after upsetting at r = 10%, 20%, 30% and 50%.

Figure 5 depicts the variation of hardness mapping with increasing r for pure titanium and β-titanium wire works. Due to low frictional state on the contact interface, the bulging deformation is suppressed to homogenize the inner strain. In both works, low hardness is limited to free bulging surfaces and highest hardness at their center is less than 270 HV. In particular, when using the β-titanium wires, the homogeneous straining takes place from r = 10% with little hardness difference

of 50 to 60 HV between the bulging surfaces and the center of works. This significantly homogeneous straining process proves that little work hardening takes place in correspondence to low interfacial stress in Table 2.

Characterization on the carbon supersaturated SKD11 punch after upsetting. What drives this low friction on the contact interface and suppresses the work hardening process is investigated by the SEM-EDX analysis on the contact interface between the cs-SKD11 punch and the β-titanium wire-work.

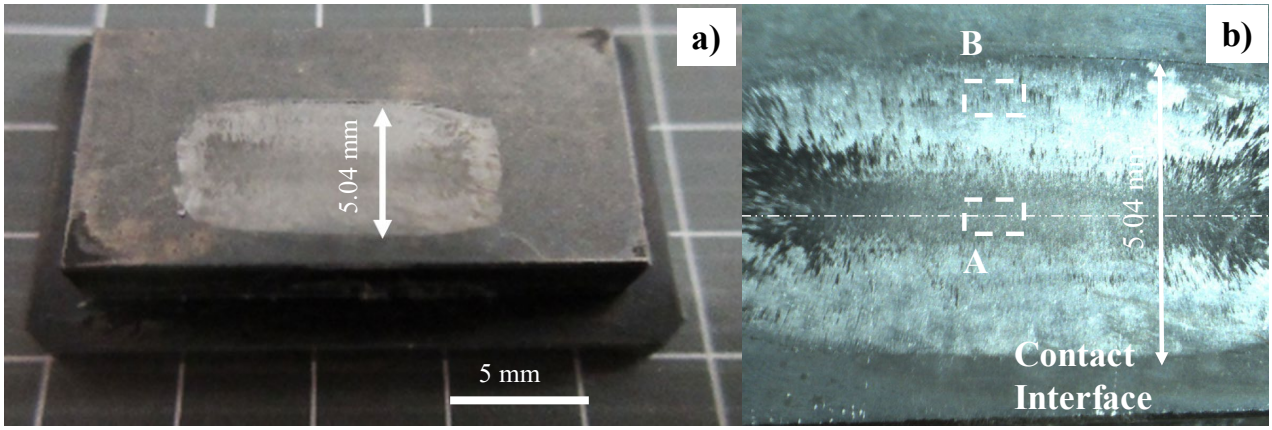

Figure 6. The cs-SKD11 punch after continuously upsetting the β-titanium wires with the diameter of 3 mm. a) Overview of the cs-SKD11 punch, and b) its contact interface to β-titanium wires.

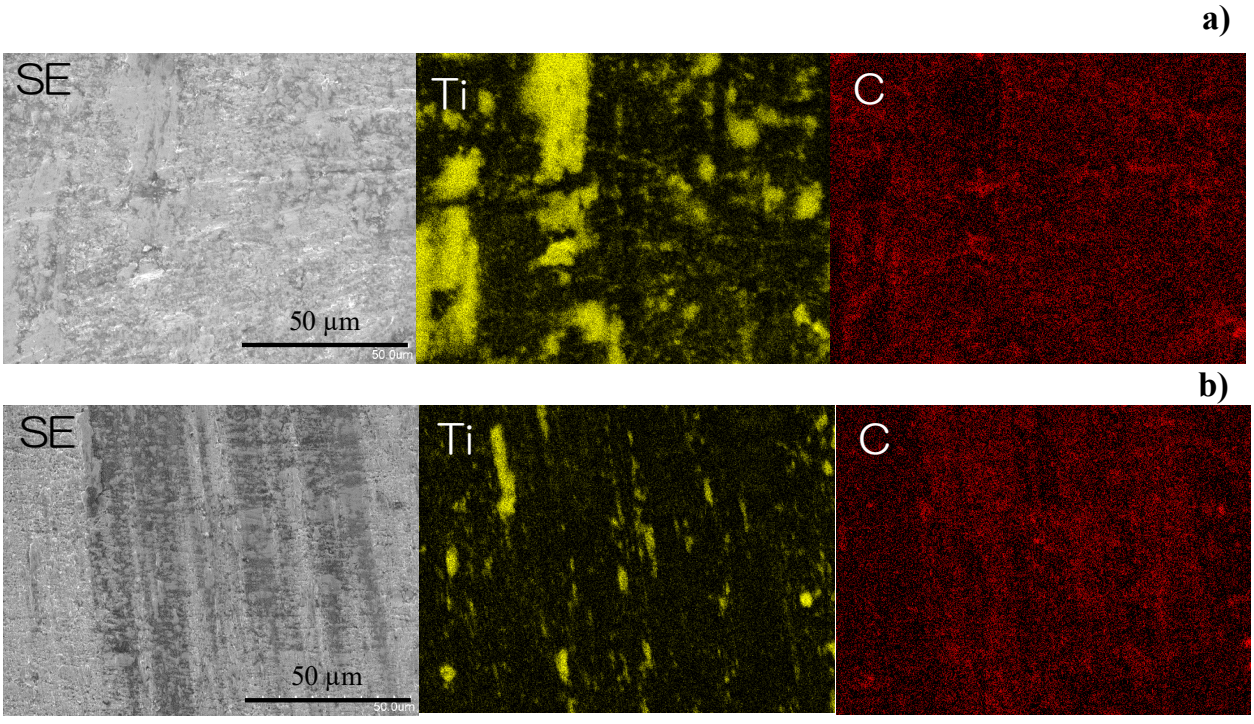

Figure 7. SEM-EDX images on the contact interface. a) A-region in Figure 6b, and b) B-region in Figure 6b.

A true contact interface was traced on the punch head surface, as depicted in Figure 6a. This trace is composed of two regions in Figure 6b. A black-colored part is formed at the center of interface; this region is dispersive in the radial direction from the centerline. This A-region is sandwiched by the gay-colored B-regions. These two regions were analyzed by SEM-EDX. As shown in Figure 7a, a few thin metallic islands with the size of 50 mm were formed; titanium mapping taught these thin films were transferred from the titanium work. Since the original Cr/Fe carbides were detected below these titanium debris films, the film thickness must be less than 0.1 µm. On other interface than those

films, the free carbon stripes distributed; the black colored agglomerates are made from these free carbon stripes.

On the B-regions, very few titanium debris films are seen in Figure 7b. After carbon mapping, the most of interface is covered by the carbon stripes. These solid lubricating tribofilm grows radially from the centerline to the ends of contact interface.

This SEM-EDX analysis on the contact interface in Figure 7, proves that the isolated free carbon tribofilm is formed on the interface for in situ solid lubrication to prevent the cs-SKD11 punch and die from severe adhesion of metallic titanium debris fragments after continuously forging with a high reduction thickness by 58%.

Near-net forging of β-titanium wires. An original b-titanium wire with the length of 80 mm was incrementally forged with the reduction of thickness by 45% to form a triangular bar by using the cs-SKD11 punch and core-die. Figure 8 compares the forged triangular car with the original wire.

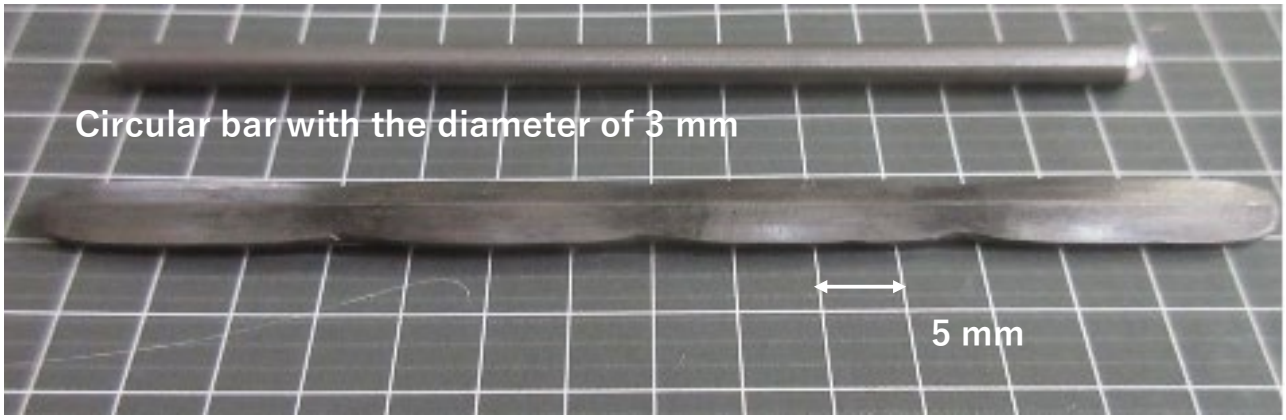

Figure 8. Incremental free near-net shaping from a b-titanium wire with the diameter of 3 mm to a triangular bar at r = 45%.

Summary

The galling-free forging with higher reduction of thickness than 40% is put into practice with the use of the carbon-supersaturated SKD11 punch and die. The in situ formation of isolated carbon tribofilms from the carbon-supersaturated SKD11 dies onto the contact interface, prevents the punch and die surface from deposition of metallic titanium and titanium oxide debris fragments. Owing to the in situ solid lubrication process, the raw β-titanium work is near-net forged with low friction and low work hardening.

Acknowledgements

The authors would like to express their gratitude to Mr. S-I. Kurozumi (Nano-Film Coat, llc.) for his help in experiments.

References

[1] B. Shirvani, R. Clarke, J. Duflou, M. Merklein, F. Micari, J. Griffiths, Stamping of titanium sheets. Key Engineering Materials 410-411 (2009) 279-288.

[2] M. Clauss, S. Graf, S. Gersbach, B. Hintermann, T. Ilchmann, M. Knupp, Material and biofilm load of K wires in toe surgery: Titanium versus stainless steel. Clin. Orthop. Relat. Res. 471 (2013) 2312–2317.

[3] https://lynskeyperformance.com/ (Retrieved at 2021/10/09).

[4] T. N. Pornsin-sirirak, Y. C. Tai, H. Nassef, C. M. Ho, Titanium-alloy MEMS wing technology for a micro aerial vehicle application. Sensors & Actuators A: Physical 89 (1-2) (2001) 95-103.

[5] T. Kihara, Visualization of deforming process of titanium and titanium alloy using high speed camera. In Proceedings of the 2019 JSTP Conference (2019) 41–42.

[6] T. Aizawa, K-I. Itoh, T. Fukuda, SiC-coated SiC die for galling-free forging of pure titanium. Mater. Trans. 61 (2) (2020) 282-288.

[7] T. Aizawa, T. Yoshino, T. Shiratori, K. Dohda, Anti-galling β -SiC coating dies for fine cold forging of titanium. J. Physics: Conference Series 1777 (2021) 012043.

[8] T. Aizawa, T. Yoshino, K-I. Ito, T. Fukuda, Thick β -SiC CVD-coated SiC die system for dry cold forging of metals. J. Crystals 10, 529 (2020) 1-13.

[9] T. Aizawa, T. Yoshino, T. Fukuda, T. Shiratori, Dry cold forging of pure titanium wire to thin plate with use of β -SiC coating dies. J. Materials 13, 3780 (2020) 1-11.

[10] T. Aizawa, K-I. Ito, T. Fukuda, Galling-free micro-forging of titanium wire with high reduction in thickness by β -SiC dies. Forming the Future, The Minerals, Metals & Materials Soc. (2021) 1065-1075.

[11] T. Aizawa, K-I. Ito, T. Fukuda, Dense SiC coating die-technology for galling-free forging process. Proc. 1 GRGLMM (Toyoma, Japan; January, 2021) 81-86.

[12] T. Aizawa, In-situ solid lubrication in cold dry forging of titanium by isolated free carbon from carbon- supersaturated dies. Proc. 7th WTC (France, Lyon, 2022, July) (in press).

[13] T. Aizawa, T. Yoshino, Y. Suzuki, T. Shiratori, Anti-galling cold, dry forging of pure titanium by plasma-carburized AISI420J2 dies. J. Appl. Sci. 11, 595 (2021) 1-12.

[14] T. Aizawa, T. Yoshino, Y. Suzuki, T. Shiratori, Free-forging of pure titanium with high reduction of thickness by plasma-carburized SKD11 dies. J. Materials 14, 2536 (2021) 1-12.

[15] T. Aizawa, T. Yoshino, T. Shiratori, Galling-free cold forging of β-titanium alloys by the plasma carburized SKD11 dies. Proc. 13th AWMFT/ASPTS (2021, November; Shanhai, China) (in press).

[16] S. Ishiguro, T. Aizawa, T. Shiratori, Characterization on the forged titanium and titanium alloys by carbon supersaturated SKD11 punch. Proc. 13th AWMFT/ASPTS (2021, November; Shanhai, China) (in press).

[17] J. J. Hong, W. C. Yeh, Application of response surface methodology to establish friction model of upset forging. Adv. Mech. Eng. 10 (2018) 1–9.

[18] S. M. Walley, Shear localization: a historical overview. Metall. Mater. Trans. A 38 (2007) 2629-2654.